Chemical Science

ROYAL SOCIETY OF CHEMISTRY

EDGE ARTICLE

View Article Online
View Journal

Cite this: DOI: 10.1039/d5sc08569a

All publication charges for this article have been paid for by the Royal Society of Chemistry

Abiotic formation of nitrile precursors to amino acids and nucleobases in interstellar ice analogues

Jia Wang, [ab] Shiori Inada,†[ab] Chaojiang Zhang,[ab] Joshua H. Marks,[ab] Zesen Wang,[ab] Alexandre Bergantini, ‡[ab] Mason McAnally, [ab] André K. Eckhardt *[c] and Ralf I. Kaiser *[ab]

Amino acids and the five canonical nucleobases have been identified in carbonaceous meteorites such as Murchison and Murray; however, their formation mechanisms under interstellar conditions have remained largely elusive. Here, we report the synthesis of biorelevant nitriles, key precursors to amino acids and nucleobases, in low-temperature interstellar model ices composed of hydrogen cyanide (HCN) irradiated with galactic cosmic ray proxies in the form of energetic electrons. Ammonia (NH_3), diazene (HNNH), methylamine (CH_3NH_2), ammonium cyanide (NH_4CN), ethanimine (CH_3CHNH), and nitriles including isocyanogen (CNCN), cyanamide (NH_2CN), iminoacetonitrile (HNCHCN), *N*-cyanomethanimine (H_2CNCN), and methyl cyanamide (CH_3NHCN) were identified utilizing vacuum ultraviolet photoionization reflectron time-of-flight mass spectrometry combined with Fourier-transform infrared spectroscopy and quadrupole mass spectrometry. These results suggest that previously astronomically undetected diazene, ammonium cyanide, and methyl cyanamide represent suitable targets for future astronomical searches. Furthermore, our findings provide fundamental insights into the non-equilibrium formation pathways leading to nitrogen-bearing molecules including complex nitriles in HCN-rich interstellar ices, thereby advancing our understanding of the abiotic origins of amino acids and nucleobases in extraterrestrial environments.

Received 4th November 2025
Accepted 4th January 2026

DOI: 10.1039/d5sc08569a

rsc.li/chemical-science

Introduction

Since the pioneering detection of hydrogen cyanide (HCN, **1**) in the interstellar medium (ISM) by Snyder and Buhl more than half a century ago,[1] nitriles – molecules containing the –C≡N functional group – have drawn sustained interest from the astrophysics,[2–4] astrochemistry,[5–7] physical chemistry,[8,9] and astrobiology communities[10,11] due to their fundamental role in the prebiotic synthesis of biomolecules linked to the Origins of Life (Fig. 1).[12–15] As of now, some seventy nitriles have been identified in the ISM (Fig. S1) ranging from simple molecules such as **1** to complex rings such as cyanocoronene ($C_{24}H_{11}CN$).[16] These nitriles account for 20% of the 354 known inter- and circumstellar molecules[17] and serve as key precursors for the abiotic synthesis of amino acids, nucleobases (purines and pyrimidines), along with nucleotides as molecular building blocks of proteins, ribonucleic acid (RNA), and deoxyribonucleic acid (DNA), respectively.[18,19] Recent analyses of returned samples from the carbonaceous asteroid Bennu revealed substantial quantities of amino acids and all five canonical nucleobases present in RNA and DNA,[20] indicating that such biorelevant molecules can form in extraterrestrial environments during the early stages of the evolution of the Solar System and may have been delivered to the early Earth by comets and meteorites.[21] In fact, amino acids such as glycine (NH_2CH_2COOH, **2**), purines like adenine ($C_5H_5N_5$, **3**) and guanine ($C_5H_5N_5O$, **4**), and pyrimidines such as uracil ($C_4H_4N_2O_2$) have been identified in key meteorites including Murchison.[22,23] Laboratory simulations have revealed the presence of nucleobases including **3** in the organic residues produced through ultraviolet (UV) irradiation of interstellar ice analogues, as verified by high-performance liquid chromatography coupled with high-resolution mass spectrometry.[24] Nevertheless, our understanding of the interstellar formation mechanisms of these biorelevant compounds, and the role of nitrile intermediates in their synthesis, remains in its infancy.

In prebiotic chemistry, **1** is considered the simplest representative of a nitrile and readily forms biorelevant building blocks including amino acids and nucleobases through oligomerization and hydrolysis reactions (Fig. 1).[10,12,15,18,25] A critical

[a]*W. M. Keck Research Laboratory in Astrochemistry, University of Hawaii at Manoa, Honolulu, Hawaii 96822, USA. E-mail: ralfk@hawaii.edu*

[b]*Department of Chemistry, University of Hawaii at Manoa, Honolulu, Hawaii 96822, USA*

[c]*Lehrstuhl für Organische Chemie II, Ruhr-Universität Bochum, Bochum 44801, Germany. E-mail: Andre.Eckhardt@ruhr-uni-bochum.de*

† Present address: Department of Basic Science, The University of Tokyo, 3-8-1 Komaba, Tokyo 153-8902, Japan

‡ Present address: Valongo Observatory, Federal University of Rio de Janeiro-UFRJ, Rio de Janeiro 20080-090, Brazil

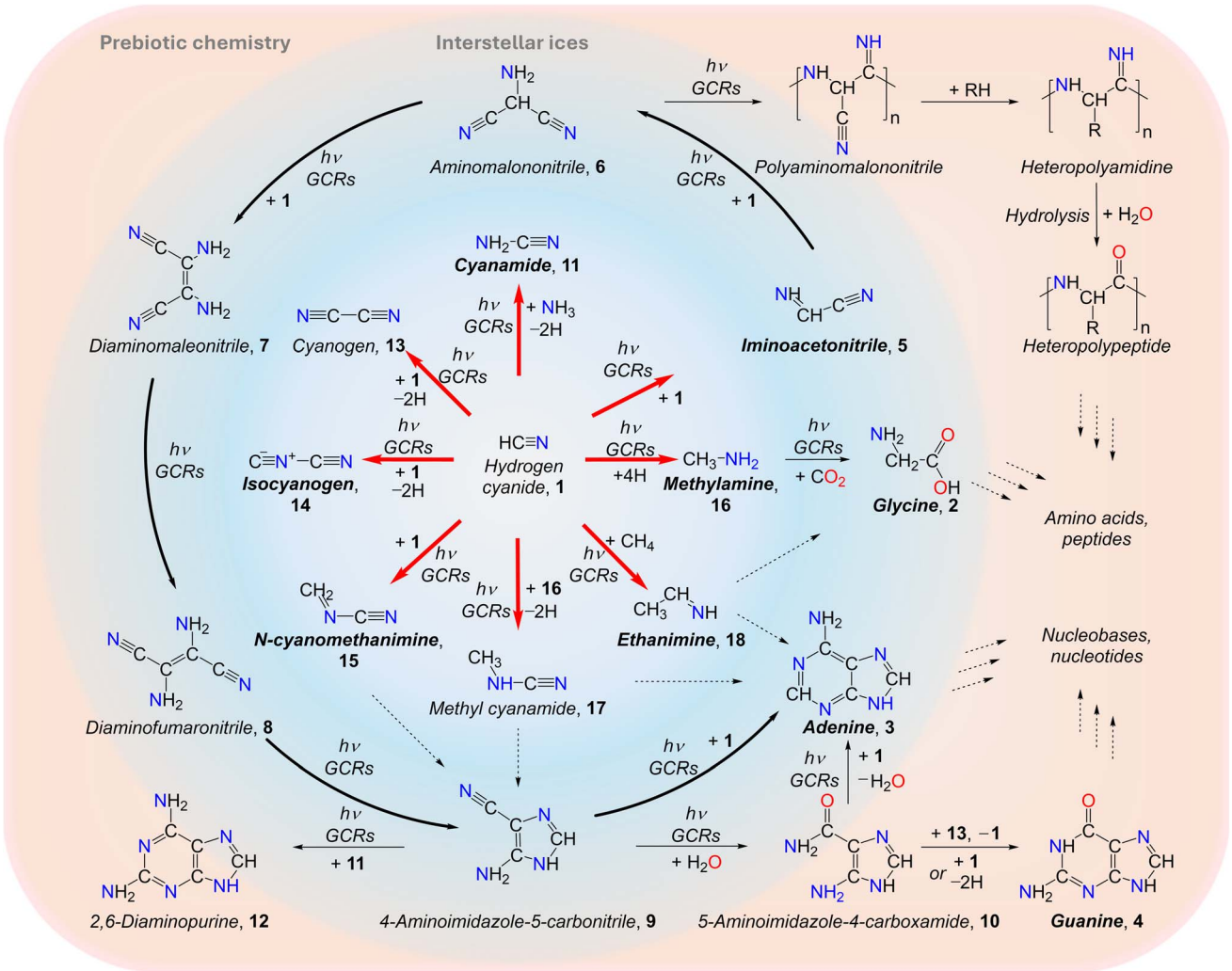

Fig. 1 Proposed formation pathways of biorelevant molecules (red arrows) in hydrogen cyanide (HCN)-containing interstellar ices and their role as precursors to biorelevant molecules such as amino acids and nucleobases. In prebiotic chemistry, hydrogen cyanide (**1**) plays a fundamental role in the synthesis of amino acids such as glycine (**2**) and nucleobases including adenine (**3**) (bold black arrows) and guanine (**4**) through non-equilibrium chemistry. Notably, **5**, **11**, **14–16**, and **18** have been detected in the interstellar medium; **2–4** have been identified in carbonaceous asteroid Bennu and various chondrites like Murchison meteorite.

step in the oligomerization cascade is the dimerization of **1** to form iminoacetonitrile (HNCHCN, **5**),[26] followed by trimerization to aminomalononitrile ($NH_2CH(CN)_2$, **6**) and subsequent tetramer ($C_4H_4N_4$) formation yielding diaminomaleonitrile (**7**), diaminofumaronitrile (**8**), and 4-aminoimidazole-5-carbonitrile (**9**).[27] Compound **6** can undergo polymerization to form polyaminomalononitrile,[13] which further transforms into heteropolyamidines that hydrolyze to heteropolypeptides leading to amino acids and peptides.[28] Condensation of **6** with formamidine ($NHCHNH_2$) accesses **9**, whereas **7** undergoes photochemical isomerization to its *trans* isomer **8**, which subsequently cyclizes to **9**.[29] Hydrolysis of **9** produces 4-aminoimidazole-5-carboxamide (**10**), which can react with **1** to form **4**; both **9** and **10** further react with **1** to yield **3**, leading to nucleobases and nucleotides.[25,30] Moreover, **9** reacts with cyanamide (NH_2CN, **11**) to form the nucleobase analog 2,6-diaminopurine ($C_5H_6N_6$, **12**), which has been detected in carbonaceous chondrites such as Murchison and Lonewolf Nunataks 94102.[31] The reaction between two **1** molecules may also generate cyanogen (NCCN, **13**), isocyanogen (CNCN, **14**), and *N*-cyanomethanimine (H_2CNCN, **15**), which serve as precursors to **3** and **9**. Stepwise hydrogenation of **1** produces methylamine (CH_3NH_2, **16**), which can further react with **1** to yield methyl cyanamide (CH_3NHCN, **17**) or with carbon dioxide (CO_2) to form the simplest proteinogenic amino acid, **2**. Upon ionizing irradiation, **1** may also react with ammonia (NH_3) and methane (CH_4) to produce **11** and ethanimine (CH_3CHNH, **18**), respectively, which are precursors to **2** and **3**. Therefore, **1** serves as a fundamental molecular building block and a key entry point in the abiotic synthesis of biorelevant molecules.[9] Elucidating the formation pathways of these compounds from **1** under interstellar conditions is crucial for understanding the astrochemical processes leading to the synthesis of astrobiologically relevant molecules, which can underpin the

emergence of prebiotic chemistry and, ultimately, the molecular Origins of Life. However, experimental evidence of these reaction pathways under astrophysical conditions has remained largely unexplored.

Here, we report the first synthesis of biorelevant nitriles in low-temperature interstellar analog ices composed of hydrogen cyanide (**1**) exposed to energetic electrons followed by their detection through isomer-selective vacuum ultraviolet (VUV) photoionization reflectron time-of-flight mass spectrometry (PI-ReToF-MS). The exploited electrons simulate secondary electrons generated by galactic cosmic rays (GCRs)[32] as they penetrate interstellar ices on nanoparticles (grains) in cold molecular clouds at typical temperatures of 5 to 10 K. The irradiation conditions correspond to GCR exposure over timescales of $(3.0 \pm 0.5) \times 10^7$ years equivalent to an evolved stage of a molecular cloud.[33] Ammonia, iminoacetonitrile (**5**), cyanamide (**11**), *N*-cyanomethanimine (**15**), methylamine (**16**), methyl cyanamide (**17**), ethanimine (**18**), and diazene (HNNH, **19**) were identified in the gas phase during temperature-programmed desorption (TPD) of the irradiated ices based on their adiabatic ionization energies (IEs) and desorption profiles. Additionally, isocyanogen (**14**), ammonium cyanide (NH_4CN, **20**), and HCN polymers were identified using Fourier-transform infrared (FTIR) spectroscopy combined with electron impact quadrupole mass spectrometry (QMS). These results provide fundamental knowledge for our understanding of how biorelevant nitriles – key precursors to amino acids and nucleobases – can form in the interstellar environments. Molecule **1** is ubiquitous in the gas phase across diverse interstellar environments including molecular clouds,[1] star-forming regions,[34,35] and protoplanetary disks,[36] with abundances up to 10^{-6} relative to molecular hydrogen (H_2).[37] It has also been observed in the atmospheres of outer planets and their moons,[38,39] in cometary comae,[40] and in the Murchison meteorite.[41] Although hydrogen cyanide (**1**) has not yet been detected in interstellar ices, it has been tentatively identified on Triton[42] and is considered a component of cometary ices.[43] Laboratory experiments have also demonstrated its solid-phase formation *via* irradiation of methane–nitrogen (CH_4–N_2) ices with ionizing radiation under astrophysically relevant conditions.[44] Therefore, our results suggest that these nitriles can likely form in **1**-containing interstellar ices in cold molecular clouds through GCR-mediated non-equilibrium chemistry. As molecular clouds evolve toward star formation, these compounds can sublimate

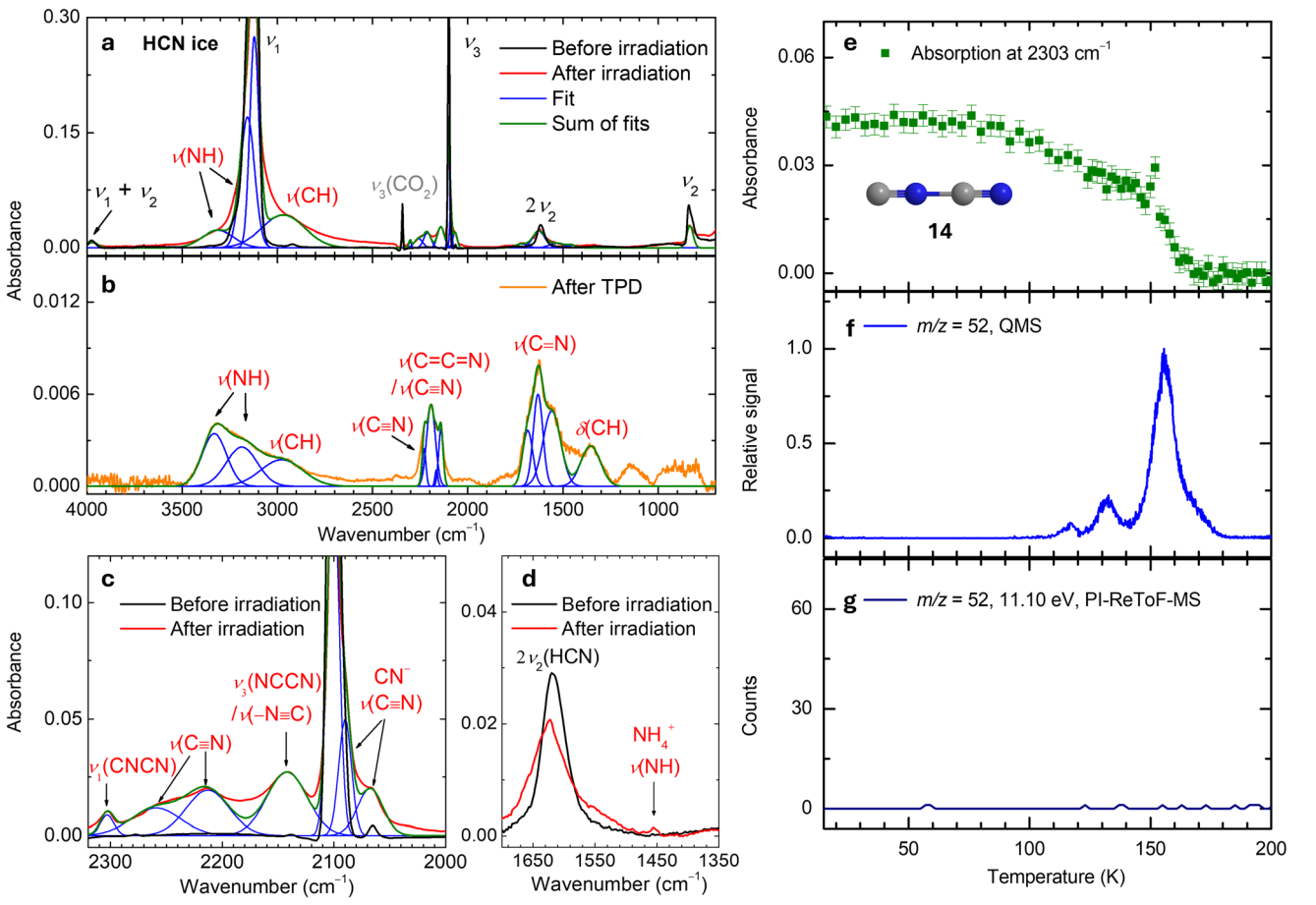

Fig. 2 Fourier transform infrared spectra (FTIR) and ion signals of $m/z = 52$ for hydrogen cyanide (**1**) ices. FTIR spectra are shown before and after irradiation at 5 K (a), with magnified view of 2320–2000 cm^{-1} (c) and 1700–1350 cm^{-1} (d) regions, and after TPD at 320 K (b). Labels indicate stretching (ν) and bending (δ) modes. (e) Temperature-dependent integrated signal at 2303 cm^{-1}. Temperature-programmed desorption (TPD) profiles of $m/z = 52$ recorded by quadrupole mass spectrometer (QMS) (f) and PI-ReToF-MS at 11.10 eV (g).

into the gas phase and represent suitable targets for future astronomical detections. Indeed, ammonia,[45] iminoacetonitrile (**5**),[46] cyanamide (**11**),[47] isocyanogen (**14**),[48] *N*-cyanomethanimine (**15**),[4] methylamine (**16**),[49] and both (*E*)- and (*Z*)-ethanimine (**18**)[50] have been detected in the ISM. Once synthesized in interstellar ices, these organics may undergo further reactions to form biorelevant molecules (Fig. 1), become incorporated into planetesimals, and ultimately be delivered to planets such as early Earth, thereby serving as key precursors to biomolecules essential for the emergence of life.[51]

Results

Infrared spectroscopy

Fourier-transform infrared (FTIR) spectra of hydrogen cyanide (**1**) ices were recorded *in situ* before, during, and after electron irradiation at 5 K (Fig. 2), with detailed assignments listed in Table S1. The observed absorptions at 3118 (ν_1, C–H stretch), 2100 (ν_3, C≡N stretch), 841 (ν_2, HCN bend), and 3977 ($\nu_1 + \nu_2$) cm^{-1} correspond to the fundamental and combination modes of **1**.[2] Upon irradiation, several new absorption features emerged. The spectra were deconvoluted into multiple Gaussian peaks. Absorptions at 3312 and 3161 cm^{-1} are linked to N–H stretching, while the absorption at 2978 cm^{-1} corresponds to C–H stretching.[52] The absorptions at 2259 and 2213 cm^{-1} are attributed to C≡N stretching (Fig. 2c),[52] which may be linked to methyl cyanamide (**17**).[53] The peak at 2142 cm^{-1} can be attributed to the C≡N asymmetric stretch of cyanogen (ν_3, **13**)[54] and/or –N≡C function group.[52] Notably, the absorption at 2303 cm^{-1} is connected to the C≡N symmetric stretch of isocyanogen (ν_1, **14**);[55] this assignment is further confirmed by the detection of the ion signals of mass-to-charge (m/z) of 52, as discussed below. Additionally, absorptions at 2090 and 2068 cm^{-1} are assigned to C≡N stretching of the cyanide anion (CN^-)[43] (Fig. 2c) and can be associated to ammonium cyanide (**20**) (Fig. S2). This conclusion is supported by the N–H stretching band of the ammonium ion (NH_4^+) observed at 1454 cm^{-1} (Fig. 2d).[56,57] After TPD at 320 K, the FTIR spectrum of the residue from irradiated **1** (Fig. 2b) matches previously measured spectra of 'poly-HCN',[43,58] confirming the formation of HCN polymers. Interestingly, although phosphine (PH_3) has a similar structure to NH_3, it is less nucleophilic. To probe the thermal reaction between PH_3 and HCN under astrophysical conditions, a separate experiment was conducted using PH_3–HCN ice mixture deposited at 10 K. Infrared spectra of the ice were recorded during TPD, but no additional absorptions features corresponding to reaction products were observed (Fig. S3), indicating that no thermal reaction occurs between PH_3 and HCN at temperatures below 136 K, at which both reactants sublimate. Overall, with the exception of small molecules like **14** and **20**, extensive spectral overlap among absorption features renders FTIR spectroscopy insufficient for the unambiguous identification of individual complex organics including nitriles. Therefore, a more sensitive, isomer-selective analytical technique is required to detect specific reaction products.

Mass spectrometry

Photoionization reflectron time-of-flight mass spectrometry (PI-ReToF-MS) was employed to identify specific isomers in the gas phase during TPD of electron-irradiated **1** ices based on their IEs and characteristic desorption temperatures.[59] This method has the unique ability to identify structural isomers based on their distinct ionization energies (IE) and/or photoionization efficiency curves (PIE).[60] Independent experiments were carried out at photon energies o f 11.10, 10.49, 9.34, and 7.60 eV to selectively ionize product isomers. The PI-ReToF-MS data obtained during TPD of the irradiated **1** ices are compiled in Fig. S4. The following sections present the TPD profiles of the ion signals corresponding to the detected products.

Ammonia. The lowest-mass observed product is ammonia (NH_3) at m/z = 17 (Fig. 3a). At a photon energy of 10.49 eV, ammonia (IE = 10.070 ± 0.020 eV)[61] can be ionized, yielding a broad sublimation event centered at 281 K. This event is absent at 9.34 eV, where ammonia cannot be ionized, thus confirming its identification. The relatively high desorption temperature of ammonia in the present study compared to pure ammonia at 108 K[62] indicates that ammonia molecules are trapped within the ice/polymer matrix and are released *via* cosublimation with higher-mass species. A blank experiment conducted under identical conditions at 10.49 eV but without electron irradiation showed no ion signal at m/z = 17, confirming that the sublimation event results from electron-induced chemical processing of **1** ices.

Diazene. At 10.49 eV, the ion signal at m/z = 30 exhibits a broad sublimation event centered at 276 K (Fig. 3b). This feature originates from C_2H_6 and/or H_2N_2 isomers. Since ethane (C_2H_6, IE = 11.52 ± 0.04 eV)[61] cannot be ionized at 10.49 eV, the observed signal therefore arises from H_2N_2 isomers—*trans*-diazene (**19**; IE = 9.61 ± 0.01 eV), *cis*-diazene (IE = 9.64 ± 0.01 eV), and/or *iso*-diazene (IE = 8.66 ± 0.01 eV).[63] In the gas phase, **19** is the most stable isomer, whereas *iso*-diazene is the least stable, lying 101 kJ mol^{-1} above **19**.[63] Upon lowering the photon energy to 9.34 eV, where only **19** (IE = 9.61 ± 0.01 eV) and *cis*-diazene (IE = 9.64 ± 0.01 eV) cannot be ionized, the sublimation event disappears, suggesting that the ion signal of m/z = 30 is attributed to *trans*- and/or *cis*-diazene. A photoionization efficiency (PIE) curve was recorded over the photon energy range 9.61–9.93 eV. Fig. 3g shows the integrated ion intensity as a function of photon energy, collected from 201 to 279 K during TPD of the irradiated ice. The experimental PIE curve agrees well with the reference PIE of *trans*-diazene (**19**).[64] Since no measured PIE curve of *cis*-diazene was reported, a contribution from *cis*-diazene cannot be ruled out as they may exhibit similar PIE curves. Therefore, the ion signal at m/z = 30 can be assigned to *trans*- and/or *cis*-diazene.

Methylamine. The ion signal at m/z = 31 is assigned to methylamine (CH_3NH_2, **16**; IE = 8.9 ± 0.1 eV),[61] the simplest primary amine. At 10.49 eV, the TPD profile exhibits a sublimation event peaking at 273 K (Fig. 3c). This desorption feature persists when the photon energy is lowered to 9.34 eV but vanishes at 7.60 eV, which is below the IE of **16**. These results confirm the identification of methylamine (**16**).

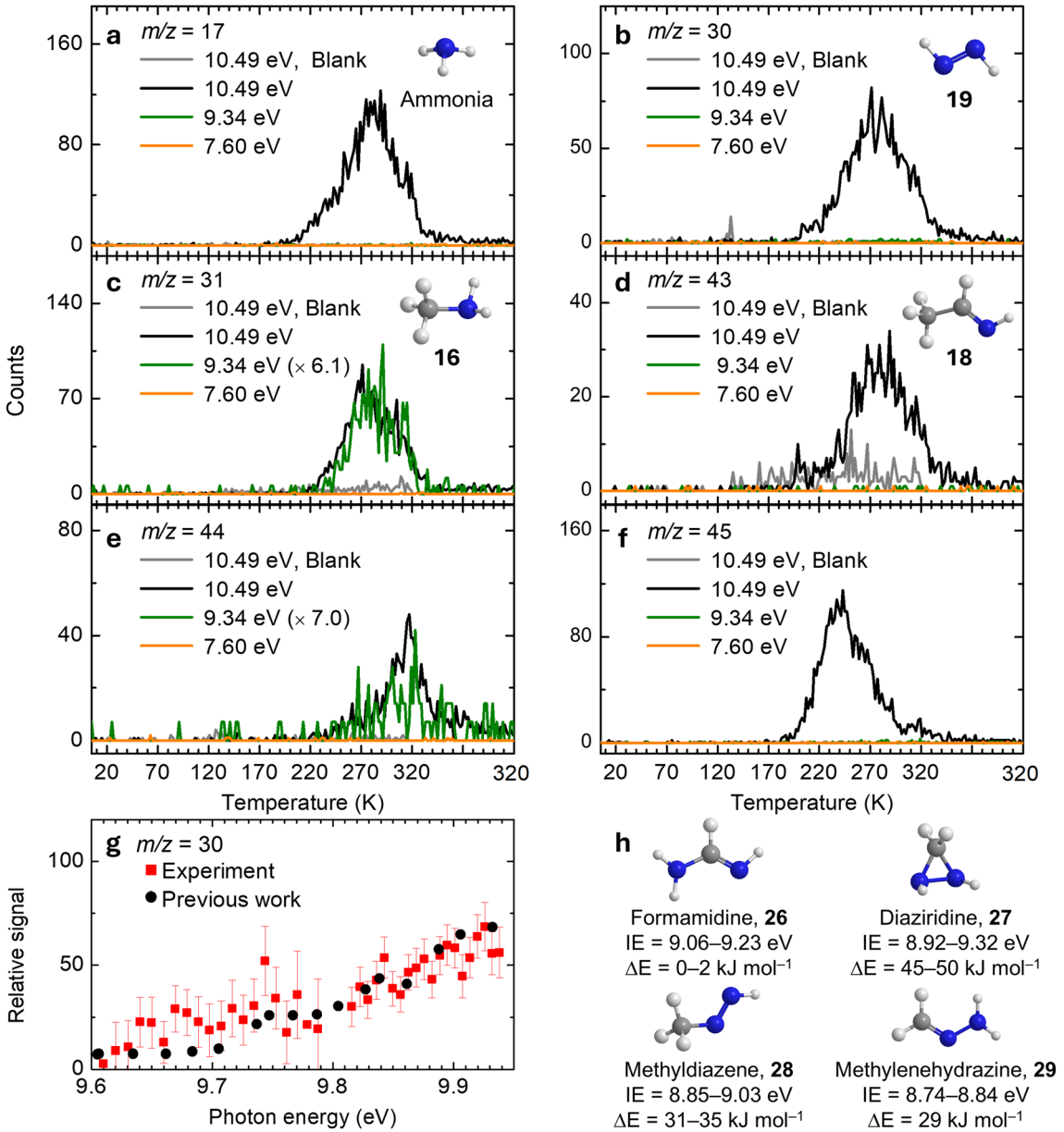

Fig. 3 Ion signals of hydrogen cyanide (**1**) ices during TPD and photoionization efficiency (PIE) curves. TPD profiles of hydrogen cyanide (**1**) ices at $m/z = 17$ (a), 30 (b), 31 (c), 43 (d), 44 (e), and 45 (f) recorded at photon energies of 10.49, 9.34, and 7.60 eV. (g) PIE curve of $m/z = 30$ plotted as a function of photon energy after correcting for the TPD profile measured from 201 to 279 K. The reference PIE curve of *trans*-diazene (**19**, black dots) is scaled for comparison with the experimental results. (h) Computed IEs and relative energies of CH_4N_2 isomers calculated at the CCSD(T)/CBS//B3LYP/aug-cc-pVTZ level of theory.

Ethanimine. The ion signal at $m/z = 43$ (Fig. 3d) belongs to molecules with molecular formula(e) HN_3 and/or C_2H_5N. Both HN_3 isomers—hydrazoic acid (HN_3, IE = 10.62–10.77 eV) and 1*H*-triazirine (*c*-HN_3, IE = 11.10–11.15 eV)[65]—cannot be ionized at 10.49 eV, indicating that the observed TPD profile originates from C_2H_5N isomers. Possible candidates include ethanimine (**18**, IE = 9.44–9.53 eV), aziridine (*c*-CH_2CH_2NH, IE = 9.23–9.31 eV), *N*-methylmethanimine (CH_2NCH_3, IE = 9.05–9.13 eV), and/or vinylamine (CH_2CHNH_2, IE = 8.05–8.13 eV).[66] When the photon energy is reduced to 9.34 eV, at which only **18** cannot be ionized, the sublimation event disappears, indicating that the ion signal at $m/z = 43$ is associated with ethanimine (**18**).

CH_4N_2 and N_3H_3 isomers. At 10.49 eV, the TPD profile of $m/z = 44$ exhibits a broad sublimation event peaking at 317 K (Fig. 3e). This signal can be attributed to molecular formula(e) C_3H_8 and/or CH_4N_2. The only C_3H_8 isomer, propane (IE = 10.94 ± 0.05 eV),[61] cannot be ionized at 10.49 eV, thus excluding any contribution. Therefore, the TPD profile of $m/z = 44$ is assigned to CH_4N_2 isomers, which includes formamidine (NH_2CHNH, **26**; IE = 9.06–9.23 eV), diaziridine (*c*-$NHCH_2NH$, **27**; IE = 8.92–9.32 eV), methyldiazene (CH_3NNH, **28**; IE = 8.85–9.03 eV), and/or methylenehydrazine (CH_2NNH_2, **29**; IE = 8.74–8.84 eV) (Fig. 3h). Upon lowering the photon energy to 9.34 eV, at which all CH_4N_2 isomers can still be ionized, the sublimation event

remains as a weak signal, indicating its origin from **26–28** and/or **29**. For the ion signal at m/z = 45, a sublimation event centered at 243 K is observed at 10.49 eV but disappears at 9.34 eV (Fig. 3f). This signal could originate from C_2H_7N and N_3H_3 isomers. However, the two possible C_2H_7N isomers—ethylamine ($CH_3CH_2NH_2$, IE = 8.81–8.96 eV) and dimethylamine (CH_3NHCH_3, IE = 8.20–8.24 eV)—should still be ionizable at 9.34 eV. The absence of ion signal at 9.34 eV therefore rules out their formation. Therefore, the TPD profile of m/z = 45 is attributed to N_3H_3 isomers such as triazene (H_2NNNH, IE = 9.24–9.53 eV), triimide (NH_2NNH, IE = 9.29–9.62 eV), and/or cyclotriazane (*c*-N_3H_3, IE = 9.83–9.93 eV).[67]

Nitriles – cyanamide, isocyanogen, iminoacetonitrile, *N*-cyanomethanimine, and methyl-cyanamide. At a photon energy of 11.10 eV, the TPD profile of m/z = 42 reveals a high-intensity sublimation event peaking at 234 K and a low-intensity shoulder extending to 320 K (Fig. 4b), which can be deconvoluted into three peaks. Possible contributors include C_3H_6 and/or CH_2N_2 isomers. The C_3H_6 isomers include cyclopropane (*c*-C_3H_6, IE = 9.86 ± 0.04 eV) and propene (CH_3CHCH_2, IE = 9.73 ± 0.01 eV).[61]

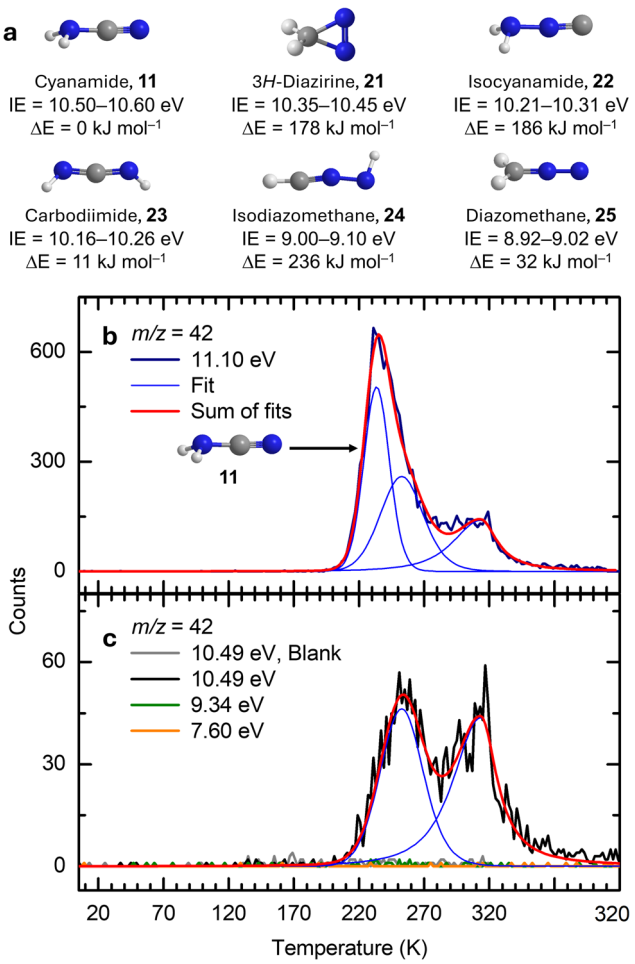

Fig. 4 Ion signals of hydrogen cyanide (**1**) ices during TPD at m/z = 42. (a) Computed IEs and relative energies of CH_2N_2 isomers calculated at the CCSD(T)/CBS//B3LYP/aug-cc-pVTZ level of theory. TPD profiles recorded at photon energies of 11.10 (b), 10.49, 9.34, and 7.60 eV (c).

The CH_2N_2 isomers comprise cyanamide (**11**, IE = 10.50–10.60 eV), 3*H*-diazirine (*c*-CH_2NN, **21**; IE = 10.35–10.45 eV), isocyanamide (NH_2NC, **22**; IE = 10.21–10.31 eV), carbodiimide (HNCNH, **23**; IE = 10.16–10.26 eV), isodiazomethane (HCNNH, **24**; IE = 9.00–9.10 eV), diazomethane (CH_2NN, **25**; IE = 8.92–9.02 eV) (Fig. 4a). Upon reducing the photon energy to 10.49 eV, the early sublimation peak at 234 K vanishes, whereas the latter two persist. Among the above isomers, only cyanamide (**11**, IE = 10.50–10.60 eV) cannot be ionized at 10.49 eV. The absence of ion signal at m/z = 42 at 10.49 eV indicates that the first sublimation event originates from cyanamide (**11**). When the photon energy is further reduced to 9.34 eV, where only **24** and **25** can be ionized, no sublimation event is observed. Therefore, the remaining sublimation events detected at 10.49 eV can be attributed to **21–23**, propene and/or cyclopropane.

Note that the QMS TPD profile at m/z = 52 obtained *via* 70 eV electron impact ionization exhibits a major sublimation event peaking at 156 K (Fig. 2f), corresponding to species with the molecular formula(e) C_4H_4 and/or C_2N_2. At 11.10 eV, all C_4H_4 isomers can be photoionized if present;[68] however, no ion signal was detected (Fig. 2g), discounting the formation of C_4H_4 isomers. Therefore, the ion signal of m/z = 52 detected by QMS can be attributed to C_2N_2 isomers—cyanogen (**13**, IE = 13.37 ± 0.01 eV),[61] isocyanogen (**14**, IE = 12.873 ± 0.005 eV),[69] and/or diisocyanogen (CNNC). Recall that **14** was identified by its C≡N symmetric stretching band at 2303 cm^{-1}.[55] The temperature-dependent integrated absorbance of this IR absorption closely correlates with the TPD profile of m/z = 52 (Fig. 2e and f), further confirming the formation of isocyanogen (**14**).

The TPD profile of the ion signal at m/z = 54 at 11.10 eV shows a broad sublimation event spanning from 160 to 320 K (Fig. 5b), which originates from molecules with formula(e) C_4H_6 and/or $C_2H_2N_2$. Given that the formation of C_4H_6 isomers from HCN requires multiple reaction steps and considering the relatively low irradiation dose used in the experiments, the production of detectable C_4H_6 isomers under our experimental conditions is unlikely. Therefore, the ion signal of m/z = 54 detected at 11.10 eV can be attributed to the $C_2H_2N_2$ isomers—iminoacetonitrile (**5**, IE = 10.87–11.00 eV) and *N*-cyanomethanimine (**15**, IE = 10.48–10.58 eV) (Fig. 5a). Upon lowering the photon energy to 10.49 eV, only **15** (IE = 10.48–10.58 eV) could be ionized, whereas **5** (IE = 10.87–11.00 eV) cannot. The ion signal of m/z = 54 at 10.49 eV exhibits a broad sublimation event between 180 and 320 K, which can be attributed to **15**. By comparing the TPD profiles at 11.10 and 10.49 eV, their difference in TPD profiles (Fig. 5c) results from the presence of **5**.

At 10.49 eV, the TPD profile of m/z = 56 exhibits a strong peak at 225 K and a lower intensity sublimation event peaking at 290 K (Fig. 6b), which arise from C_4H_8, $C_2H_4N_2$, and/or N_4 isomers. Due to the multiple reaction steps required to form C_4H_8 and N_4 isomers from HCN, the observed signal can be attributed to $C_2H_4N_2$ isomers. Possible $C_2H_4N_2$ isomers include methyl cyanamide (**17**, IE = 9.75–9.85 eV), 1,2-diiminoethane (HNCHCHNH, **30**; IE = 9.73–10.12 eV), aminoacetonitrile (NH_2CH_2CN, **31**; IE = 9.83–9.99 eV), 1,3-diaza-1,3-butadiene (CH_2NCHNH, **32**; IE = 9.26–9.40 eV), and 2,3-diaza-1,3-

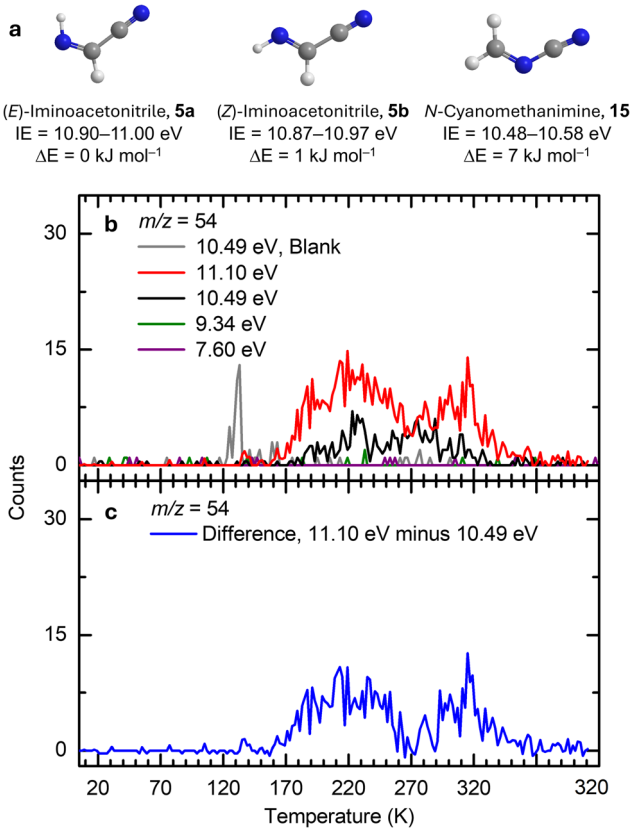

Fig. 5 Ion signals of hydrogen cyanide (**1**) ices during TPD at $m/z = 54$. (a) Computed IEs and relative energies of $C_2H_2N_2$ isomers calculated at the CCSD(T)/CBS//B3LYP/aug-cc-pVTZ level of theory. (b) TPD profiles recorded at photon energies of 11.10, 10.49, 9.34, and 7.60 eV. TPD profiles of $m/z = 54$ were each recorded twice at 11.10 eV and 10.49 eV and the difference in their averaged profiles (c).

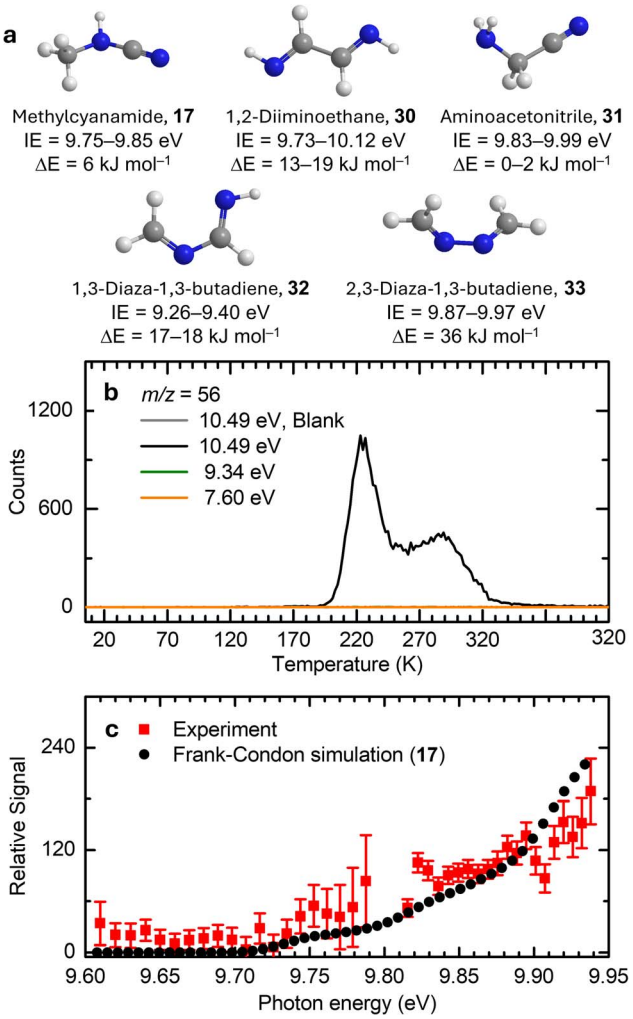

Fig. 6 Ion signals of hydrogen cyanide (**1**) ices during TPD at $m/z = 56$ and photoionization efficiency (PIE) curves. (a) Computed IEs and relative energies of $C_2H_4N_2$ isomers calculated at the CCSD(T)/CBS//B3LYP/aug-cc-pVTZ level of theory. (b) TPD profiles recorded at photon energies of 10.49, 9.34, and 7.60 eV. (c) PIE curve plotted as a function of photon energy after correcting for the TPD profile measured from 281 to 320 K. The Franck–Condon simulation of the PIE curve of methyl cyanamide (**17**, black dots) is scaled for comparison with the experimental results.

butadiene (CH_2NNCH_2, **33**; IE = 9.87–9.97 eV). When the photon energy was reduced to 9.34 eV, at which **17** (IE = 9.75–9.85 eV), **30** (IE = 9.73–10.12 eV), and **31** (IE = 9.83–9.99 eV) cannot be ionized, the sublimation events disappear, indicating that the ion signal of $m/z = 56$ is attributed to **17**, **30**, and/or **31**. To distinguish between these isomers, a PIE curve of $m/z = 56$ was recorded during TPD of irradiated ice between 281 and 320 K using photon energies from 9.61 to 9.93 eV (Fig. 6c). This PIE curve for $m/z = 56$ agrees with the predicted PIE curve of **17**, indicating the formation of **17**. The ionization onset of **17** is determined to be 9.73 ± 0.02 eV, which is close to its computed IE. Recall that the FTIR results indicate the tentative identification of the C≡N stretching of methyl cyanamide (**17**) at 2259 and 2213 cm^{-1}.[53] Notably, the computed Franck–Condon factors of the *syn* conformers of **30** (**30d** (IE = 9.91–10.01 eV), **30e** (IE = 9.84–9.94 eV) and **30f** (IE = 9.73–9.83 eV)) are significantly lower than those of the other isomers (Fig. S5), ruling out their contribution. This is consistent with a recent UV photolysis study of 1,2-diazidoethane ($C_2H_4N_6$) at 3 K in solid argon, which only revealed the formation of the three *anti* conformers **30a–30c**, while the *syn* conformers **30d–30f** remained unobserved.[70] The strong sublimation feature at 225 K partially overlaps with the TPD profile of $m/z = 68$, 69, and 83 (Fig. S6), suggesting that this event may originate from the fragments generated *via* the dissociative photoionization of these higher-mass species.

Discussion

Having provided compelling evidence for the formation of ammonia, methylamine (**16**), ethanimine (**18**), diazene (**19**), ammonium cyanide (**20**), and nitriles including iminoacetonitrile (**5**), cyanamide (**11**), isocyanogen (**14**), *N*-cyanomethanimine (**15**), and methyl cyanamide (**17**) in hydrogen cyanide (**1**) ices irradiated with GCR proxies, we now discuss their potential formation pathways (Fig. 7). First, the unimolecular decomposition of **1** produces atomic hydrogen (H) and cyano (CN) radicals *via* C–H bond cleavage (reaction (1)), which is endoergic by

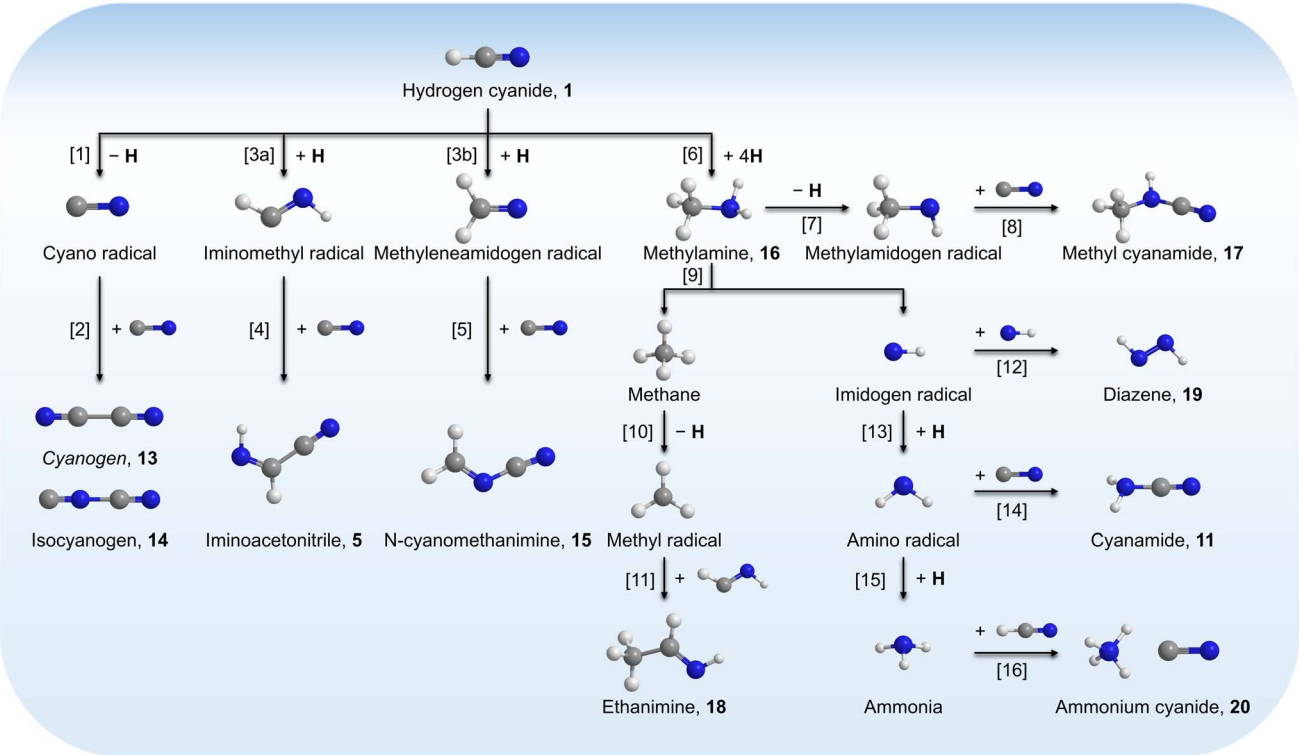

Fig. 7 Potential formation pathways of **5**, **11**, and **14–20** in irradiated hydrogen cyanide (**1**) ices. Cyanogen (**13**) is tentatively identified and indicated in italic.

523 kJ mol^{-1}.[71] This energy can be supplied by the energetic electrons, highlighting the critical role of external energy sources such as GCRs in initiating the conversion of **1** into cyano radicals in extraterrestrial ices. Two cyano radicals can subsequently react in an exoergic process to **13** *via* reaction (2a) or **14** *via* reaction (2b), either at 5 K if their recombination geometry is favorable or in the TPD phase as the radical mobility increases. Note that **13** was tentatively identified *via* FTIR by its C≡N asymmetric stretch (ν_3)[54] at 2142 cm^{-1}.

A suprathermal hydrogen atom may add to the carbon–nitrogen triple bond of **1**, forming the iminomethyl (HCNH) radical through reaction (3a) or the methyleneamidogen (H_2CN) radical *via* reaction (3b); reactions (3a) and (3b) are exoergic by 70 and 104 kJ mol^{-1}, respectively.[71] Subsequent barrierless radical–radical recombination between the cyano radical and either the iminomethyl or methyleneamidogen radical yields **5** and **15** *via* reactions (4) and (5), with energy releases of 484 and 416 kJ mol^{-1}, respectively; the overall reaction energies to **5** and **15** from two **1** molecules are −30 and +4 kJ mol^{-1}, respectively.[71,72]

$$\mathrm{HCN}(\mathbf{1}) \rightarrow \mathrm{CN} + \mathrm{H},\ \Delta H_r^\circ(0\ \mathrm{K}) = +523\ \mathrm{kJ\ mol^{-1}} \quad (1)$$

$$\mathrm{CN} + \mathrm{CN} \rightarrow \mathrm{NCCN}(\mathbf{13}),\ \Delta H_r^\circ(0\ \mathrm{K}) = -565\ \mathrm{kJ\ mol^{-1}} \quad (2a)$$

$$\mathrm{CN} + \mathrm{CN} \rightarrow \mathrm{CNCN}(\mathbf{14}),\ \Delta H_r^\circ(0\ \mathrm{K}) = -461\ \mathrm{kJ\ mol^{-1}} \quad (2b)$$

$$\mathrm{HCN}(\mathbf{1}) + \mathrm{H} \rightarrow \mathrm{HCNH},\ \Delta H_r^\circ(0\ \mathrm{K}) = -70\ \mathrm{kJ\ mol^{-1}} \quad (3a)$$

$$\mathrm{HCN}(\mathbf{1}) + \mathrm{H} \rightarrow \mathrm{H_2CN},\ \Delta H_r^\circ(0\ \mathrm{K}) = -104\ \mathrm{kJ\ mol^{-1}} \quad (3b)$$

$$\mathrm{HCNH} + \mathrm{CN} \rightarrow \mathrm{HNCHCN}(\mathbf{5}),\ \Delta H_r^\circ(298\ \mathrm{K}) = -484\ \mathrm{kJ\ mol^{-1}} \quad (4)$$

$$\mathrm{H_2CN} + \mathrm{CN} \rightarrow \mathrm{H_2CNCN}(\mathbf{15}),\ \Delta H_r^\circ(298\ \mathrm{K}) = -416\ \mathrm{kJ\ mol^{-1}} \quad (5)$$

Stepwise hydrogenation by suprathermal hydrogen atoms of **1** may form **16** *via* reaction (6). Specifically, a hydrogen atom can recombine with the iminomethyl and methyleneamidogen radicals to yield aminomethylene ($HCNH_2$), methanimine (H_2CNH),[73] and methylimidogen (H_3CN) (Fig. 8). Subsequent hydrogen-atom additions produce aminomethyl (H_2CNH_2) and methylamidogen (H_3CNH) radicals, followed by further hydrogenation leading to **16**.[74] It is worth noting that the closed-shell molecule methanimine was tentatively identified in the experiments (Fig. S7, SI). Once formed in the ices, **16** may serve as a precursor to form **17** and **18**. The unimolecular decomposition of **16** may form the methylamidogen radical (reaction (7)),[74] which can subsequently recombine with the cyano radical to form **17** through reaction (8), an exoergic process releasing 470 kJ mol^{-1}.[71,72] Alternatively, upon interaction with energetic electrons, **16** may yield imidogen radical (NH) and methane (CH_4) (reaction (9)),[75] which undergoes C–H bond cleavage to form the methyl (CH_3) radical *via* reaction (10).[76] The formation of **18** can then proceed through barrierless recombination

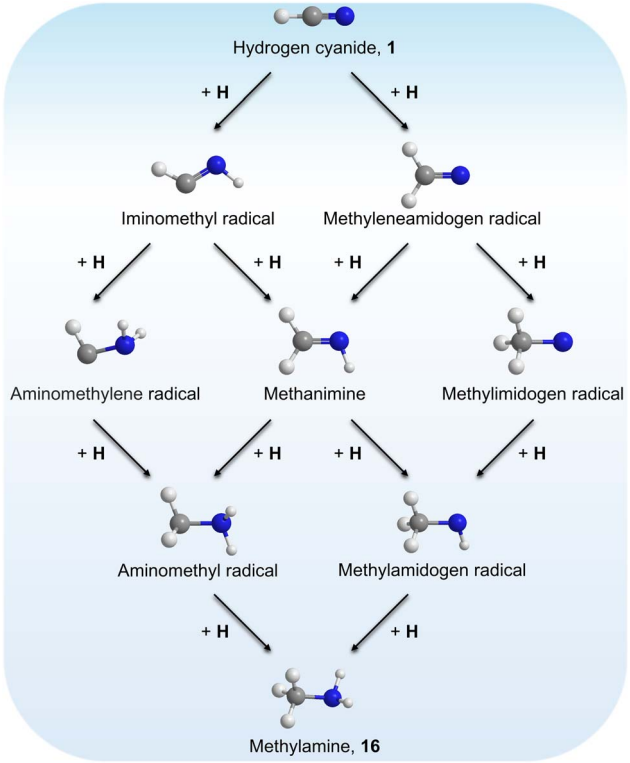

Fig. 8 Potential stepwise hydrogenation formation pathways of **16** in irradiated hydrogen cyanide (**1**) ices.

between the methyl and iminomethyl radicals *via* reaction (11), which is exoergic by 370 kJ mol^{-1}.[71]

$$HCN(\mathbf{1}) + 4H \rightarrow CH_3NH_2(\mathbf{16}),\ \Delta H_r^\circ(0\ K) = -1000\ kJ\ mol^{-1} \quad (6)$$

$$CH_3NH_2(\mathbf{16}) \rightarrow CH_3NH + H,\ \Delta H_r^\circ(0\ K) = +410\ kJ\ mol^{-1} \quad (7)$$

$$CH_3NH + CN \rightarrow CH_3NHCN(\mathbf{17}),\ \Delta H_r^\circ(298\ K) = -470\ kJ\ mol^{-1} \quad (8)$$

$$CH_3NH_2(\mathbf{16}) \rightarrow CH_4 + NH,\ \Delta H_r^\circ(0\ K) = +299\ kJ\ mol^{-1} \quad (9)$$

$$CH_4 \rightarrow CH_3 + H,\ \Delta H_r^\circ(0\ K) = +432\ kJ\ mol^{-1} \quad (10)$$

$$CH_3 + CHNH \rightarrow CH_3CHNH(\mathbf{18}),\ \Delta H_r^\circ(0\ K) = -370\ kJ\ mol^{-1} \quad (11)$$

Furthermore, barrierless self-recombination between two imidogen radicals produces **19** *via* reaction (12),[77] an exoergic process releasing 510 kJ mol^{-1}.[71] Subsequent hydrogen addition to the imidogen radical yields the amino radical (NH_2) (reaction (13)), which reacts with the cyano radical and hydrogen atom to yield **11** and ammonia through reactions (14) and (15), respectively. Reactions (12)–(15) are highly exoergic by 510, 386, 484, and 444 kJ mol^{-1}, respectively.[71] Finally, the nucleophilic addition of ammonia to **1** forms **20** *via* reaction (16) with a reaction endoergicity of 1 kJ mol^{-1}.[57,71,78] It is worth noting that future theoretical modeling of these proposed reaction pathways would be valuable to fully elucidate the underlying formation mechanisms of nitrogen-containing molecules in interstellar environments.

$$NH + NH \rightarrow HNNH(\mathbf{19}),\ \Delta H_r^\circ(0\ K) = -510\ kJ\ mol^{-1} \quad (12)$$

$$NH + H \rightarrow NH_2,\ \Delta H_r^\circ(0\ K) = -386\ kJ\ mol^{-1} \quad (13)$$

$$NH_2 + CN \rightarrow NH_2CN(\mathbf{11}),\ \Delta H_r^\circ(0\ K) = -484\ kJ\ mol^{-1} \quad (14)$$

$$NH_2 + H \rightarrow NH_3,\ \Delta H_r^\circ(0\ K) = -444\ kJ\ mol^{-1} \quad (15)$$

$$HCN(\mathbf{1}) + NH_3 \rightarrow NH_4CN(\mathbf{20}),\ \Delta H_r^\circ(298\ K) = +1\ kJ\ mol^{-1} \quad (16)$$

Conclusion and outlook

The present work demonstrates the first preparation of biorelevant nitriles in low-temperature interstellar model ices composed of hydrogen cyanide (**1**). The ices were irradiated with GCR proxies in the form of energetic electrons[32] at doses corresponding to exposure timescales equivalent to evolved stages of molecular clouds of $(3.0 \pm 0.5) \times 10^7$ years.[33] Utilizing VUV photoionization reflectron time-of-flight mass spectrometry, ammonia, iminoacetonitrile (**5**), cyanamide (**11**), *N*-cyanomethanimine (**15**), methylamine (**16**), methyl cyanamide (**17**), ethanimine (**18**), and diazene (HNNH, **19**) were identified in the gas phase during TPD of the irradiated **1** ices based on their IEs and desorption profiles. In addition, isocyanogen (**14**), ammonium cyanide (NH_4CN, **20**), and HCN polymers of undefined chemical structure were detected *via* FTIR spectroscopy combined with QMS. These results provide fundamental insights into the formation pathways leading to these nitrogen-bearing molecules in **1**-rich interstellar ices through non-equilibrium chemistry, representing a critical step toward understanding how nitrile precursors to amino acids and nucleobases can be synthesized under astrophysical conditions.

Notably, hydrogen cyanide (**1**) is a ubiquitous molecule in the ISM, with abundances reaching up to 10^{-6} relative to molecular hydrogen in the hot envelope;[37] it has been detected in the gas phase in various environments including molecular clouds,[1,79] star-forming regions,[34,35] shocked regions,[80] and protoplanetary disks.[36] Although **1** has not yet been identified in interstellar ices, solid-phase **1** has been tentatively detected on Triton[42] and is considered a component of cometary ices.[43] Therefore, our results suggest that ammonia, **5**, **11**, **14**–**20**, and HCN polymers can plausibly form in **1**-containing interstellar ices within cold molecular clouds upon exposure to ionizing radiation such as GCRs. As molecular clouds evolve into star-forming regions, these compounds may sublimate into the gas phase[32] and represent promising targets—especially for the hitherto undetected **17**, **19**, and **20**—for future astronomical detections towards star-forming regions using radio telescopes such as the Atacama Large Millimeter/submillimeter Array

(ALMA). Additionally, once synthesized in interstellar ices, these compounds may serve as key precursors to fundamental biomolecules such as glycine (**2**), adenine (**3**), and guanine (**4**) (Fig. 1), providing plausible abiotic pathways toward the synthesis of amino acids and nucleobases under extraterrestrial conditions. In fact, **2–4** have been identified in carbonaceous chondrites such as Murchison,[22,23] suggesting that such biomolecules could have been delivered to the early Earth and contributed to the emergence of Life.

It is worth noting that the hydrogen cyanide (**1**) ices used in this work serve as a simple model system to investigate how biorelevant nitriles can form upon exposure to GCR proxies. Our experiments represent an initial step towards elucidating their fundamental formation mechanisms in a controlled environment. Considering that interstellar ices are composed primarily of water along with minor molecules such as carbon dioxide, carbon monoxide (CO), and methanol (CH_3OH),[81] future laboratory simulation experiments incorporating these molecules into **1** ices may reveal additional pathways to nitriles and other products. For instance, the irradiated water–**1** and carbon dioxide–**1** ices may eventually lead to the formation of **4** and **2**, respectively (Fig. 1); the inclusion of carbon monoxide or methanol into **1** ices may yield cyanoformaldehyde (HOCCN) and glycolonitrile ($HOCH_2CN$), respectively, which have been identified in the ISM.[82,83] These experiments may further advance our understanding of the role of hydrogen cyanide chemistry in the abiotic formation of biorelevant molecules *via* non-equilibrium reactions in deep space.

Lastly, the absence of new absorption features during TPD of the unirradiated PH_3–HCN ice mixture indicates that no thermal reaction occurs between PH_3 and HCN during the warm-up phase of star formation. This thermal inertness arises from the lower nucleophilicity of PH_3 relative to NH_3. Phosphorus has lower electronegativity ($\chi(P) = 2.46$ and $\chi(N) = 2.93$)[84] and a larger atomic radius (99 pm) relative to nitrogen (54 pm),[85] leading to a more diffuse lone pair on phosphorus and reducing its ability to engage electrophiles in an ice matrix. Moreover, P–N and P–C bonds are generally weaker than the corresponding N–N and N–C bonds, which makes the formation of new P–N or P–C linkages thermodynamically less favorable and increases the barriers for addition to nitriles. Additionally, previous laboratory simulation experiments have demonstrated the efficient formation of biorelevant phosphorus-containing molecules in interstellar ices *via* radical–radical recombination and insertion reactions initiated by energetic processing.[86–88] These findings suggest that the formation of complex phosphorus-containing molecules in interstellar ices requires non-equilibrium, energy-driven chemistry initiated by ionizing sources such as GCRs or UV photons, providing a crucial constraint for astrochemical models. Notably, cyanophosphine (PH_2CN) has been searched for toward Sagittarius B2(N) with an abundance upper limit of 7.0×10^{-12} relative to molecular hydrogen.[89] Future experiments could investigate the formation of H_2PCN isomers through electron irradiation of PH_3–HCN ice mixtures, as cyanophosphine may form through recombination between the phosphino (PH_2) and cyano (CN) radicals.

Author contributions

R. I. K. designed and conceptualized the experiments; J. W., S. I., C. Z., J. H. M., Z. W., A. B., and M. M. performed the experiments; J. W. and S. I. analyzed the data; A. K. E. conducted the theoretical analysis; and J. W., A. K. E., and R. I. K. wrote the manuscript.

Conflicts of interest

The authors declare no conflicts of interest.

Data availability

Essential data are provided in the main text and the supplementary information (SI). Additional data are available from the corresponding author upon reasonable request. Supplementary information: experimental and computational methods, other mass channels and their tentative assignments, known interstellar CN-containing molecules (Fig. S1), FTIR spectra of NH_3–HCN and PH_3–HCN ices (Fig. S2 and S3) and assignments (Tables S1 and S2), PI-ReToF-MS data of irradiated HCN ices (Fig. S4), calculated Franck–Condon factors (Fig. S5), TPD profiles of other mass channels from irradiated HCN ice (Fig. S6, S7 and S9, S10), resonance-enhanced multiphoton ionization (REMPI) spectroscopy measurements for nitrogen monoxide (Fig. S8), experimental conditions (Table S3), VUV photon generation parameters (Table S4), error analysis of IEs and relative energies (Tables S5–S8), and Cartesian coordinates, vibrational frequencies, and infrared intensities of computed structures (Tables S9–S12). See DOI: https://doi.org/10.1039/d5sc08569a.

Acknowledgements

This study was supported by the U.S. National Science Foundation (NSF), Division of Astronomical Sciences, under grant AST-2403867 to the University of Hawaii at Manoa (R. I. K). The calculations in Bochum were funded by the Deutsche Forschungsgemeinschaft (DFG, German Research Foundation) under Germany's Excellence Strategy – EXC 2033 – 390677874 – RESOLV (A. K. E).

References

1 L. E. Snyder and D. Buhl, *Astrophys. J.*, 1971, **163**, L47.
2 P. A. Gerakines, Y. Y. Yarnall and R. L. Hudson, *Mon. Not. R. Astron. Soc.*, 2021, **509**, 3515–3522.
3 R. L. Hudson and P. A. Gerakines, *Planet. Sci. J.*, 2023, **4**, 205.
4 D. San Andrés, V. M. Rivilla, L. Colzi, I. Jiménez-Serra, J. Martín-Pintado, A. Megías, Á. López-Gallifa, A. Martínez-Henares, S. Massalkhi, S. Zeng, M. Sanz-Novo, B. Tercero, P. de Vicente, S. Martín, M. A. Requena Torres, G. Molpeceres and J. García de la Concepción, *Astrophys. J.*, 2024, **967**, 39.

5 J. A. Noble, P. Theule, F. Borget, G. Danger, M. Chomat, F. Duvernay, F. Mispelaer and T. Chiavassa, *Mon. Not. R. Astron. Soc.*, 2012, **428**, 3262–3273.
6 T. J. Hager, B. M. Moore, Q. D. Borengasser, K. T. Renshaw, R. Johnson, A. C. Kanaherarachchi and B. M. Broderick, *ACS Earth Space Chem.*, 2025, **9**, 2137–2147.
7 F. Izquierdo-Ruiz, M. L. Cable, R. Hodyss, T. H. Vu, H. Sandström, A. Lobato and M. Rahm, *Proc. Natl. Acad. Sci. U. S. A.*, 2025, **122**, e2507522122.
8 M. Xie, X. Sun, W. Li, J. Guan, Z. Liang and Y. Hu, *J. Phys. Chem. Lett.*, 2022, **13**, 8207–8213.
9 R. Santalucia, M. Pazzi, F. Bonino, M. Signorile, D. Scarano, P. Ugliengo, G. Spoto and L. Mino, *Phys. Chem. Chem. Phys.*, 2022, **24**, 7224–7230.
10 M. Ruiz-Bermejo, M.-P. Zorzano and S. Osuna-Esteban, *Life*, 2013, **3**, 421–448.
11 P. B. Rimmer and O. Shorttle, *Life*, 2024, **14**, 498.
12 J. OrÓ, *Nature*, 1961, **191**, 1193–1194.
13 C. N. Matthews and R. D. Minard, *Faraday Discuss.*, 2006, **133**, 393–401.
14 M. d'Ischia, P. Manini, M. Moracci, R. Saladino, V. Ball, H. Thissen, R. A. Evans, C. Puzzarini and V. Barone, *Int. J. Mol. Sci.*, 2019, **20**, 4079.
15 J. D. Sutherland, *Angew. Chem., Int. Ed.*, 2016, **55**, 104–121.
16 G. Wenzel, S. Gong, C. Xue, P. B. Changala, M. S. Holdren, T. H. Speak, D. A. Stewart, Z. T. P. Fried, R. H. J. Willis, E. A. Bergin, A. M. Burkhardt, A. N. Byrne, S. B. Charnley, A. Lipnicky, R. A. Loomis, C. N. Shingledecker, I. R. Cooke, M. C. McCarthy, A. J. Remijan, A. E. Wendlandt and B. A. McGuire, *Astrophys. J., Lett.*, 2025, **984**, L36.
17 D. E. Woon, *The Astrochymist*, 2025, http://www.astrochymist.org/, accessed October 10, 2025.
18 J. OrÓ and S. S. Kamat, *Nature*, 1961, **190**, 442–443.
19 S. Becker, J. Feldmann, S. Wiedemann, H. Okamura, C. Schneider, K. Iwan, A. Crisp, M. Rossa, T. Amatov and T. Carell, *Science*, 2019, **366**, 76–82.
20 D. P. Glavin, J. P. Dworkin, C. M. O. D. Alexander, J. C. Aponte, A. A. Baczynski, J. J. Barnes, H. A. Bechtel, E. L. Berger, A. S. Burton, P. Caselli, A. H. Chung, S. J. Clemett, G. D. Cody, G. Dominguez, J. E. Elsila, K. K. Farnsworth, D. I. Foustoukos, K. H. Freeman, Y. Furukawa, Z. Gainsforth, H. V. Graham, T. Grassi, B. M. Giuliano, V. E. Hamilton, P. Haenecour, P. R. Heck, A. E. Hofmann, C. H. House, Y. Huang, H. H. Kaplan, L. P. Keller, B. Kim, T. Koga, M. Liss, H. L. McLain, M. A. Marcus, M. Matney, T. J. McCoy, O. M. McIntosh, A. Mojarro, H. Naraoka, A. N. Nguyen, M. Nuevo, J. A. Nuth, Y. Oba, E. T. Parker, T. S. Peretyazhko, S. A. Sandford, E. Santos, P. Schmitt-Kopplin, F. Seguin, D. N. Simkus, A. Shahid, Y. Takano, K. L. Thomas-Keprta, H. Tripathi, G. Weiss, Y. Zheng, N. G. Lunning, K. Righter, H. C. Connolly and D. S. Lauretta, *Nat. Astron.*, 2025, **9**, 199–210.
21 S. Kwok, *Int. J. Astrobiol.*, 2009, **8**, 161–167.
22 P. G. Stoks and A. W. Schwartz, *Nature*, 1979, **282**, 709–710.
23 Y. Oba, Y. Takano, Y. Furukawa, T. Koga, D. P. Glavin, J. P. Dworkin and H. Naraoka, *Nat. Commun.*, 2022, **13**, 2008.
24 Y. Oba, Y. Takano, H. Naraoka, N. Watanabe and A. Kouchi, *Nat. Commun.*, 2019, **10**, 4413.
25 M. Yadav, R. Kumar and R. Krishnamurthy, *Chem. Rev.*, 2020, **120**, 4766–4805.
26 H. Sandström and M. Rahm, *ACS Earth Space Chem.*, 2021, **5**, 2152–2159.
27 C. Grundke, C. Kong, C. J. Kampf, B. F. Gupton, D. T. McQuade and T. Opatz, *J. Org. Chem.*, 2021, **86**, 10320–10329.
28 M. Ruiz-Bermejo, J. L. de la Fuente, C. Pérez-Fernández and E. Mateo-Martí, *Processes*, 2021, **9**, 597.
29 R. Sanchez, J. Ferris and L. E. Orgel, *Science*, 1966, **153**, 72–73.
30 J. C. Choe, *Chem. Phys. Lett.*, 2018, **708**, 71–76.
31 M. P. Callahan, K. E. Smith, H. J. Cleaves, J. Ruzicka, J. C. Stern, D. P. Glavin, C. H. House and J. P. Dworkin, *Proc. Natl. Acad. Sci. U. S. A.*, 2011, **108**, 13995–13998.
32 J. Wang, C. Zhang, J. H. Marks, M. M. Evseev, O. V. Kuznetsov, I. O. Antonov and R. I. Kaiser, *Nat. Commun.*, 2024, **15**, 10189.
33 A. G. Yeghikyan, *Astrophysics*, 2011, **54**, 87–99.
34 P. Schilke, C. M. Walmsley, G. Pineau Des Forets, E. Roueff, D. R. Flower and S. Guilloteau, *Astron. Astrophys.*, 1992, **256**, 595–612.
35 M. Jin, J.-E. Lee and K.-T. Kim, *Astrophys. J., Suppl. Ser.*, 2015, **219**, 2.
36 D. Graninger, K. I. Öberg, C. Qi and J. Kastner, *Astrophys. J., Lett.*, 2015, **807**, L15.
37 F. Lahuis and E. F. van Dishoeck, *Astron. Astrophys.*, 2000, **355**, 699–712.
38 A. T. Tokunaga, S. C. Beck, T. R. Geballe, J. H. Lacy and E. Serabyn, *Icarus*, 1981, **48**, 283–289.
39 J. S. Peter, T. A. Nordheim and K. P. Hand, *Nat. Astron.*, 2024, **8**, 164–173.
40 M. Agúndez, N. Biver, P. Santos-Sanz, D. Bockelée-Morvan and R. Moreno, *Astron. Astrophys.*, 2014, **564**, L2.
41 S. Pizzarello, *Astrophys. J., Lett.*, 2012, **754**, L27.
42 M. Burgdorf, D. P. Cruikshank, C. M. Dalle Ore, T. Sekiguchi, R. Nakamura, G. Orton, E. Quirico and B. Schmitt, *Astrophys. J., Lett.*, 2010, **718**, L53.
43 P. A. Gerakines, M. H. Moore and R. L. Hudson, *Icarus*, 2004, **170**, 202–213.
44 C. S. Jamieson, A. H. H. Chang and R. I. Kaiser, *Adv. Space Res.*, 2009, **43**, 1446–1450.
45 A. C. Cheung, D. M. Rank, C. H. Townes, D. D. Thornton and W. J. Welch, *Phys. Rev. Lett.*, 1968, **21**, 1701–1705.
46 D. P. Zaleski, N. A. Seifert, A. L. Steber, M. T. Muckle, R. A. Loomis, J. F. Corby, O. Martinez, K. N. Crabtree, P. R. Jewell, J. M. Hollis, F. J. Lovas, D. Vasquez, J. Nyiramahirwe, N. Sciortino, K. Johnson, M. C. McCarthy, A. J. Remijan and B. H. Pate, *Astrophys. J., Lett.*, 2013, **765**, L10.
47 B. E. Turner, H. S. Liszt, N. Kaifu and A. G. Kisliakov, *Astrophys. J.*, 1975, **201**, L149–L152.
48 M. Agúndez, N. Marcelino and J. Cernicharo, *Astrophys. J., Lett.*, 2018, **861**, L22.

49 N. Kaifu, M. Morimoto, K. Nagane, K. Akabane, T. Iguchi and K. Takagi, *Astrophys. J.*, 1974, **191**, L135–L137.
50 R. A. Loomis, D. P. Zaleski, A. L. Steber, J. L. Neill, M. T. Muckle, B. J. Harris, J. M. Hollis, P. R. Jewell, V. Lattanzi, F. J. Lovas, O. Martinez, M. C. McCarthy, A. J. Remijan, B. H. Pate and J. F. Corby, *Astrophys. J.*, 2013, **765**, L9.
51 C. Chyba and C. Sagan, *Nature*, 1992, **355**, 125–132.
52 G. Socrates, *Infrared and raman characteristic group frequencies: Tables and charts*, John Wiley & Sons, Ltd, New York, 3rd edn., 2004.
53 M. Pagacz-Kostrzewa, J. Krupa and M. Wierzejewska, *J. Photochem. Photobiol., A*, 2014, **277**, 37–44.
54 R. J. Blanch and A. McCluskey, *Chem. Phys. Lett.*, 1995, **241**, 116–120.
55 F. Stroh and M. Winnewisser, *Chem. Phys. Lett.*, 1989, **155**, 21–26.
56 J. R. Brucato, G. A. Baratta and G. Strazzulla, *Astron. Astrophys.*, 2006, **455**, 395–399.
57 P. A. Gerakines, Y. Y. Yarnall and R. L. Hudson, *Icarus*, 2024, **413**, 116007.
58 B. N. Khare, C. Sagan, W. R. Thompson, E. T. Arakawa, C. Meisse and P. S. Tuminello, *Can. J. Chem.*, 1994, **72**, 678–694.
59 A. M. Turner and R. I. Kaiser, *Acc. Chem. Res.*, 2020, **53**, 2791–2805.
60 J. Wang, A. A. Nikolayev, J. H. Marks, A. M. Turner, S. Chandra, N. F. Kleimeier, L. A. Young, A. M. Mebel and R. I. Kaiser, *J. Am. Chem. Soc.*, 2024, **146**, 28437–28447.
61 S. G. Lias, Ionization Energy Evaluation, in *NIST Chemistry WebBook, NIST Standard Reference Database Number 69*, ed. P. J. Linstrom and W. G. Mallard, National Institute of Standards and Technology, Gaithersburg MD, 20899, DOI: 10.18434/T4D303, accessed October 1, 2025.
62 S. K. Singh, A. Bergantini, C. Zhu, M. Ferrari, M. C. De Sanctis, S. De Angelis and R. I. Kaiser, *Nat. Commun.*, 2021, **12**, 1–8.
63 A. M. Turner, Y. Luo, J. H. Marks, R. Sun, J. T. Lechner, T. M. Klapötke and R. I. Kaiser, *J. Phys. Chem. A*, 2022, **126**, 4747–4761.
64 B. Ruscic and J. Berkowitz, *J. Chem. Phys.*, 1991, **95**, 4378–4384.
65 C. Zhang, C. Zhu, A. K. Eckhardt and R. I. Kaiser, *J. Phys. Chem. Lett.*, 2022, **13**, 2725–2730.
66 C. Zhang, J. Wang, A. M. Turner, J. H. Marks, S. Chandra, R. C. Fortenberry and R. I. Kaiser, *Astrophys. J.*, 2023, **952**, 132.
67 M. Förstel, Y. A. Tsegaw, P. Maksyutenko, A. M. Mebel, W. Sander and R. I. Kaiser, *ChemPhysChem*, 2016, **17**, 2726–2735.
68 J. Wang, J. H. Marks, A. K. Eckhardt and R. I. Kaiser, *J. Phys. Chem. Lett.*, 2024, **15**, 1211–1217.
69 O. Grabandt, C. A. De Lange, R. Mooyman, T. Van Der Does and F. Bickelhaupt, *Chem. Phys. Lett.*, 1989, **155**, 221–226.
70 A. K. Eckhardt, *Chem. Commun.*, 2022, **58**, 8484–8487.
71 B. Ruscic and H. Bross, *Active Thermochemical Tables (ATcT) values based on ver. 1.130 of the Thermochemical Network, ATcT.anl.gov*, 2021.
72 G. Leroy, J.-P. Dewispelaere, C. Wilante and H. Benkadour, *Macromol. Theory Simul.*, 1997, **6**, 729–739.
73 C. Zhu, R. Frigge, A. M. Turner, M. J. Abplanalp, B.-J. Sun, Y.-L. Chen, A. H. Chang and R. I. Kaiser, *Phys. Chem. Chem. Phys.*, 2019, **21**, 1952–1962.
74 J. H. Marks, J. Wang, R. C. Fortenberry and R. I. Kaiser, *Proc. Natl. Acad. Sci. U. S. A.*, 2022, **119**, e2217329119.
75 J. O. Thomas, K. E. Lower and C. Murray, *J. Phys. Chem. Lett.*, 2012, **3**, 1341–1345.
76 C. J. Bennett, C. S. Jamieson, Y. Osamura and R. I. Kaiser, *Astrophys. J.*, 2006, **653**, 792–811.
77 E. Mullikin, P. van Mulbregt, J. Perea, M. Kasule, J. Huang, C. Buffo, J. Campbell, L. Gates, H. M. Cumberbatch, Z. Peeler, H. Schneider, J. Lukens, S. T. Bao, R. Tano-Menka, S. Baniya, K. Cui, M. Thompson, A. Hay, L. Widdup, A. Caldwell-Overdier, J. Huang, M. C. Boyer, M. Rajappan, G. Echebiri and C. R. Arumainayagam, *ACS Earth Space Chem.*, 2018, **2**, 863–868.
78 N. Luft, *Ind. Chem.*, 1955, **31**, 502–504.
79 B. E. Turner, L. Pirogov and Y. C. Minh, *Astrophys. J.*, 1997, **483**, 235.
80 B. Lefloch, G. Busquet, S. Viti, C. Vastel, E. Mendoza, M. Benedettini, C. Codella, L. Podio, A. Schutzer, P. R. Rivera-Ortiz, J. R. D. Lépine and R. Bachiller, *Mon. Not. R. Astron. Soc.*, 2021, **507**, 1034–1046.
81 K. I. Öberg, *Chem. Rev.*, 2016, **116**, 9631–9663.
82 A. J. Remijan, J. M. Hollis, F. J. Lovas, W. D. Stork, P. R. Jewell and D. S. Meier, *Astrophys. J.*, 2008, **675**, L85.
83 S. Zeng, D. Quénard, I. Jiménez-Serra, J. Martín-Pintado, V. M. Rivilla, L. Testi and R. Martín-Doménech, *Mon. Not. R. Astron. Soc.*, 2019, **484**, L43–L48.
84 D. Bergmann and J. Hinze, *Angew. Chem., Int. Ed. Engl.*, 1996, **35**, 150–163.
85 D. C. Ghosh and R. Biswas, *Int. J. Mol. Sci.*, 2002, **3**, 87–113.
86 A. M. Turner, A. Bergantini, M. J. Abplanalp, C. Zhu, S. Góbi, B.-J. Sun, K.-H. Chao, A. H. H. Chang, C. Meinert and R. I. Kaiser, *Nat. Commun.*, 2018, **9**, 3851.
87 C. Zhu, A. M. Turner, M. J. Abplanalp, R. I. Kaiser, B. Webb, G. Siuzdak and R. C. Fortenberry, *Astrophys. J.*, 2020, **899**, L3.
88 J. Wang, B.-J. Sun, A. Bergantini, Z. Wang, A. M. Turner, A. H. H. Chang and R. I. Kaiser, *J. Am. Chem. Soc.*, 2025, **147**, 38987–38991.
89 D. T. Halfen, D. J. Clouthier and L. M. Ziurys, *Astrophys. J.*, 2014, **796**, 36.